Biosensors and Bioelectronics 86 (2016) 690–696

Contents lists available at ScienceDirect

Biosensors and Bioelectronics

journal homepage: www.elsevier.com/locate/bios

Detection of Hepatitis C core antibody by dual-affinity yeast chimera and smartphone-based electrochemical sensing

Eliah Aronoff-Spencer [a,*,1], A.G. Venkatesh [b,1], Alex Sun [b], Howard Brickner [a], David Looney [a,c], Drew A. Hall [b]

[a] School of Medicine, University of California, San Diego, La Jolla, CA, 92093 USA
[b] Department of Electrical and Computer Engineering, University of California, San Diego, La Jolla, CA, 92093 USA
[c] VA San Diego Healthcare System, San Diego, CA, 92161 USA

ARTICLE INFO

Article history:
Received 21 April 2016
Received in revised form
17 June 2016
Accepted 8 July 2016
Available online 9 July 2016

Keywords:
mHealth
Point-of-care diagnostics
Hepatitis C virus
Yeast biobrick
Whole cell biosensor
Electrochemical biosensor

ABSTRACT

Yeast cell lines were genetically engineered to display Hepatitis C virus (HCV) core antigen linked to gold binding peptide (GBP) as a dual-affinity biobrick chimera. These multifunctional yeast cells adhere to the gold sensor surface while simultaneously acting as a "renewable" capture reagent for anti-HCV core antibody. This streamlined functionalization and detection strategy removes the need for traditional purification and immobilization techniques. With this biobrick construct, both optical and electrochemical immunoassays were developed. The optical immunoassays demonstrated detection of anti-HCV core antibody down to 12.3 pM concentrations while the electrochemical assay demonstrated higher binding constants and dynamic range. The electrochemical format and a custom, low-cost smartphone-based potentiostat ($20 USD) yielded comparable results to assays performed on a state-of-the-art electrochemical workstation. We propose this combination of synthetic biology and scalable, point-of-care sensing has potential to provide low-cost, cutting edge diagnostic capability for many pathogens in a variety of settings.

1. Introduction

Hepatitis C Viral (HCV) infection is a global healthcare concern due to the high morbidity and mortality associated with chronic infection (Chen and Morgan, 2006; Saito et al., 1990). HCV is primarily acquired through blood transfusion or unsterilized medical needles/devices and causes chronic liver disease with strong epidemiological linkage to subsequent hepatocellular carcinoma (Saito et al., 1990). The virus undergoes a high rate of RNA mutation leading to significant genetic variations impeding vaccine development (Stoll-Keller et al., 2009) and confounding control efforts. New, highly-effective and well-tolerated direct-acting antiviral drugs (Edlin and Winkelstein, 2014; Graham and Swan, 2015) are now driving disease control efforts globally (Hagan and Schinazi, 2013), making eradication of HCV infection within a generation achievable. However, this will require identifying and treating an estimated population of 130 – 150 million mono-infected (Suthar and Harries, 2015) and 5.5 million HIV co-infected individuals (Rouet et al., 2015) worldwide. Accurate, low-cost point-of-care (POC) diagnostic devices are key to effectively screen and monitor the treatment of hundreds of millions, especially those living in resource poor settings, where both testing and treatment costs remain significant constraints (Edlin and Winkelstein, 2014; Graham and Swan, 2015).

Anti-HCV antibody and HCV RNA load testing is expected to cost $20 billion USD by the end of this decade (Uliana et al., 2014). Three generations of anti-HCV antibody tests have relied on enzyme-linked immunosorbent assay (ELISA) technology to detect viral proteins: NS4 alone in the first generation (Kuo et al., 1989); the HCV core, NS3, and NS4 in the second (Gretch, 1997); and the core, NS3, NS4, and NS5 in the third (Barrera et al., 1995; Kao et al., 1996; Uyttendaele et al., 1994). The increasing assay sensitivity of each successive generation has reduced the time to detect anti-HCV antibody from 16 to 5 weeks after initial infection (Uliana et al., 2014). The HCV core antigen remains crucial, as it highly conserved (Ribeiro et al., 2012) and the serum concentration of the protein correlates with the viral RNA concentration, allowing it to be used in as an indirect marker for viral replication (Bouvier-Alias et al., 2002; Gaudy et al., 2005; Park et al., 2010; Zanetti et al., 2003).

Recombinant HCV core proteins have been successfully expressed in a variety of host systems including bacteria (Majeau et al., 2004), yeast (Acosta-Rivero et al., 2002), mammalian cells

* Correspondence to: University of California, San Diego, 9500 Gilman Drive, La Jolla, CA 92093, USA.
E-mail address: earonoffspencer@ucsd.edu (E. Aronoff-Spencer).
[1] These authors contributed equally to this work.

http://dx.doi.org/10.1016/j.bios.2016.07.023
0956-5663/

(Harada et al., 1991), insect cells (Baumert et al., 1998), and plants (Madesis et al., 2010). While production of HCV core protein in large quantities has been realized, cultivation must be tightly controlled, purification often requires multiple steps, and immobilization on a testing substrate all combine to increase the costs and complexity of assay production. An alternative approach is illustrated by one-step purification and surface binding of human papilloma virus (HPV) L1 capsid glutathione s-transferase fusion proteins to a glutathione-casein coated ELISA plate for detection of anti-HPV antibody in human serum (Sehr et al., 2002). A chimera of viral antigen and a high affinity substrate binding moiety simplifies the production of immunologic tests. Other low-cost genetically-engineered fusion proteins have been produced in non-pathogenic *E. coli* (van Bloois et al., 2011), *S. cerevisiae*, *Lactobacillus* sp. (Qin et al., 2014), and *Bacillus sp*. (Du et al., 2005; Iwanicki et al., 2014) for a variety of diagnostic applications (Cherf and Cochran, 2015). Recently, Jaun Franco et al. (2013) reported site-directed antibody deposition for surface plasmon resonance (SPR) using protein A-gold binding domain (PAG) antibody fusion proteins. This strategy led to proteins that bound avidly and in the correct orientation to gold monolayers, and is the foundation of the current work.

Here we present a platform to detect anti-HCV core antibody combining yeast biobricks and scalable sensing methods. Yeast cells were genetically engineered to display HCV core protein concatenated to gold binding peptide (GBP) repeats, creating affinity reagents capable of self-assembly on gold surfaces. This technique enables single-step purification, surface preparation and deposition, and is compatible with a host of technologies ranging from optical imaging to electrochemical sensing. We developed and compared both optical and electrochemical assays to explore the avidity and efficiency of yeast-based reagents. Ultimately, functionalized gold screen printed electrodes (SPE) were used to detect HCV antibodies by a low-cost potentiostat yielding direct transduction of immune-complex formation into a signal that is sensed, processed, and transmitted by a smartphone (Fig. 1).

2. Materials and methods

2.1. Construction of HCV-core/GBP yeast display vectors

Yeast display vectors pYD and pCTCON2 were kindly provided by K. Dane Wittrup, MIT, MA (Wang et al., 2005) and canonical restriction sites such as *Nhe*I and *Bam*HI at *N*- and *C*-terminal respectively were added to facilitate insertion of HCV-core and GBP genes. The complete HCV-core gene was cloned by polymerase chain reaction (PCR) with forward and reverse primers consisting of *Nhe*I and *Bam*HI, respectively, from pCMV3010-HCV1, an HCV1 genome library constructed from a clinical sample. The PCR product was then restriction digested (*Nhe*I and *Bam*HI), cleaned, and ligated into pYD and pCTCON2 vectors. The DNA sequence corresponding to GBP (sequence: MHGKTQATSGTIQS) was cloned from template (Stanley, 1997) by PCR with both forward and reverse primers consisting of *Bam*HI site. The PCR product was then digested with *Bam*HI and inserted adjacent to HCV-core gene by ligation. The sequence of all vectors was confirmed by population sequencing.

2.2. Transformation and induction of yeast display vectors

The constructed vectors were transformed into *S. cerevisiae* EBY100 strain from ATCC using DSY yeast transformation kit (Dualsystems Biotech AG, #P01003). The transformed HCV-core/GBP expressing yeasts were then freshly streaked on SD+CAA selective media plates at 30 °C overnight. A fresh single colony was subsequently inoculated in 5 mL of SR+CAA media and incubated for 2 days at 30 °C, diluted to achieve 1 OD_{600}, and aliquoted in 1 mL batches. The expression was induced by inoculating 0.5 mL from 1 mL aliquots in 5 mL of S/Galactose and Raffinose+CAA media and incubated for 48 h at 20 °C. Preparation of media is described in supplementary of reference (Venkatesh et al., 2015).

2.3. Immuno-fluorescent assay for yeast display validation

100 μL galactose induced yeast cells were centrifuged in 96 well plates and re-suspended in 50 μL 1 × PBS containing 1% bovine serum albumin (BSA) and incubated at room temperature for 30 min to pre-block the surface. Mouse monoclonal anti-HCV core IgG (Santa Cruz Biotech, #sc-57800) of desired concentration was added to the yeast cells and the plate was gently rocked for 2 h at room temperature. The yeast cells were then washed 3 × with 50 μL 1 × PBS by centrifugation and resuspension. The Alexa Fluor 488 conjugated donkey anti-mouse IgG (Thermo Fischer, #A-21202) was subsequently added incubated for 1 h at room temperature followed by 3 × wash with 50 μL 1 × PBS. The pellets were then re-suspended in 20 μL 1 × PBS and measured for fluorescence using flow cytometer with suitable excitation and emission filters (BD Accuri C6).

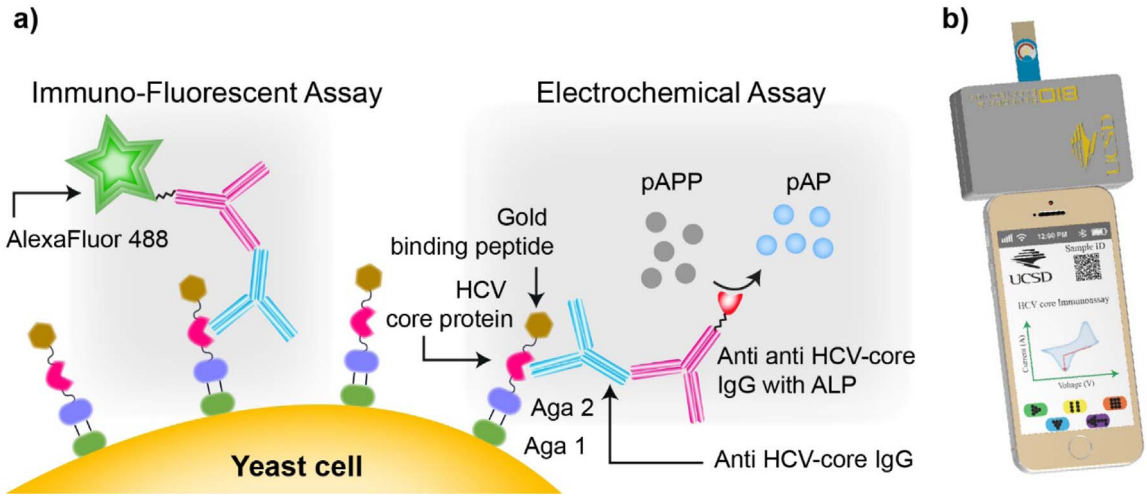

Fig. 1. Illustration of yeast biobrick chimera enabled detection of anti-HCV core antibody with POC smartphone potentiostat platform. (a) Detection of anti-HCV core antibody by fluorescence and electrochemical methods. (b) Illustration of smartphone-based potentiostat that connects to a host device through the audio jack.

2.4. Procedure for cleaning electrode

Gold SPEs from Dropsens (DRP-250AT) were cleaned with a mixture of 50 mM KOH and H_2O_2 (3:1) for 10 min to remove organics from the gold surface. The gold surface was further electrochemically cleaned in the presence of 50 mM sulfuric acid by sweeping a potential between −0.4 V to +0.4 V at a rate of 100 mV/s for 12 cycles, using a benchtop potentiostat (CH Instruments 750E). The electrode was finally rinsed with deionized water and air-blow dried.

2.5. Functionalization of gold surface with displayed HCV-core/GBP chimera

50 μL 1 OD_{600} cells grown in induction media was dropped on the clean gold surface of the electrode and incubated overnight at 4 °C. The electrodes were then rinsed with 1 mL 1 × Tris buffered saline (TBS) pH 7.4, and treated with 50 μL 1% sodium azide in 1 × TBS for 90 min at room temperature and rinsed with 1 mL TBS. The electrode chip was blocked with 1 × TBS containing 2% BSA and 0.05% TWEEN-20 for 1 h at room temperature and rinsed with 1 mL TBS.

2.6. Electrochemical sandwich ELISA

The functionalized electrode was incubated with 20 μL of mouse anti-HCV core monoclonal IgG (Santa Cruz Biotech, #sc-57800) with desired concentration for 2 h at room temperature and rinsed with 1 mL TBS. 20 μL of alkaline phosphatase (ALP) conjugated secondary IgG's from rabbit (Abcam, # ab6729) targeted towards mouse IgG was added and incubated for 1 h at room temperature. The electrode was then rinsed 3x with 1 mL TBS and air-blow dried. The immune complex formation was detected by adding 50 μL substrate solution (100 mM glycine pH 10.4, 6 mM *p*-aminophenyl phosphate (*p*APP) (Santa Cruz Biotech, #sc-281392), 1 mM $ZnCl_2$, and 1 mM $MgCl_2$) to the electrode and incubated at 37 °C for 10 min. The conversion of *p*APP to *p*-aminophenol (*p*AP) by ALP was detected by cyclic voltammetry by a potential sweep between +0.3 V to −0.25 V at a rate of 25 mV/s for 10 cycles using CHI 750E or smartphone-based potentiostat. The measured current vs antibody concentration was fitted with 4-parameter logistic regression. The limit of detection (LOD) and limit of quantification (LOQ) were calculated as the amplitude of the control sample (0 nM) plus 3σ and 10σ, respectively. The linear dynamic range (DR) was calculated from the LOQ to the upper boundary, where the calibration curve saturates, minus 10σ.

2.7. Smartphone-based potentiostat

A portable potentiostat was designed as a peripheral module that plugs directly into the headphone jack of the user's smartphone (Sun et al., 2014, 2016). The block diagram in Fig. 2a illustrates how the module harvests power through the left audio channel, communicates bi-directionally with its smartphone host via the right channel and the microphone, and makes electrochemical measurements. The smartphone provided energy to the device by sending a sinusoidal tone (5–20 kHz) that was rectified and then regulated to a 4-volt DC supply. The harvesting circuit also includes a tunable impedance matching network automated by the smartphone and completely hidden from the operator (Yao et al., 2015) to ensure optimum power transfer. For digital communication, the microcontroller in the module sent and received serial RS-232 packets across the right audio output and the microphone channels at a baud rate of 2.4 kHz. Via this communication protocol, the smartphone, once given user input, sent commands to the microcontroller to set different test parameters for cyclic voltammetry (CV) measurements, such as scan-rate (25–100 mV/s) and scan range (± 2 V) as well as to start and stop tests. Finally, the module's low-power potentiostat were interfaced with disposable screen printed electrodes plugged into the device to make CV measurements (Fig. 2b). CV operates by applying a triangular voltage waveform between the working and reference electrodes in an electrochemical cell and recording the current generated at the working electrode. In this module, the microcontroller generated the voltage ramps for the potentiostat to use and the resulting measured current signal was amplified and then transformed into a voltage by the potentiostat. Using a voltage controlled oscillator (VCO), this voltage data output by the potentiostat was first converted to a frequency signal within the audio band and then sent to the phone to be recorded, demodulated, and reconstructed (Fig. 2c). To make reconstructing the voltammogram, which is the current plotted against the input voltage of a CV measurement, easier when the smartphone is processing the data, marker tones, which signify the voltage transition points of the applied potential, were generated by the microcontroller and inserted into the output of the VCO (Fig. 2c).

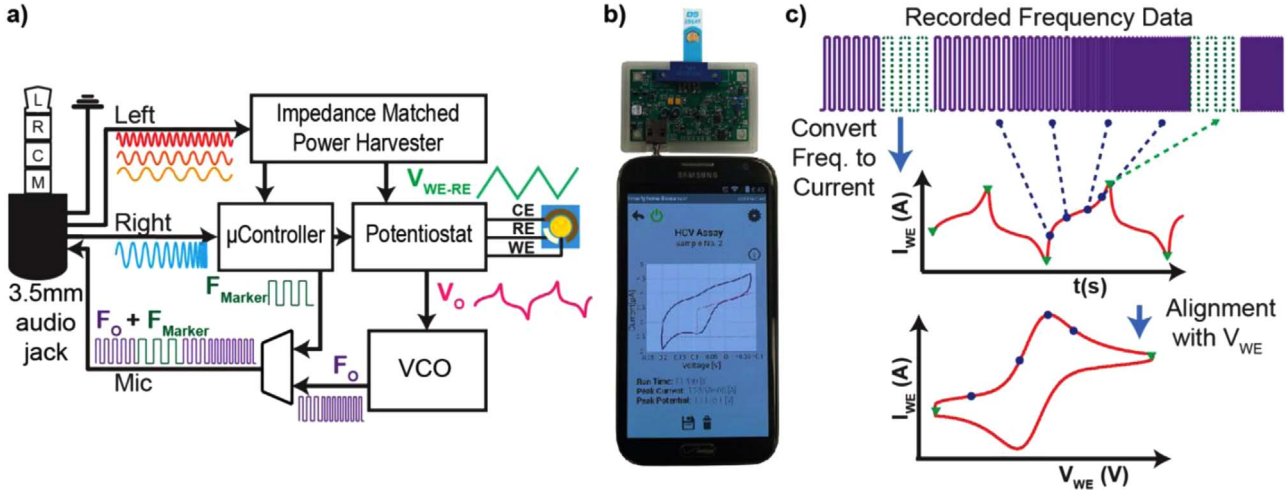

Fig. 2. POC Smartphone-based potentiostat platform: (a) Block diagram of potentiostat circuit interfaced through 3.5 mm audio jack, (b) Photograph of smartphone potentiostat measuring anti-HCV core antibody by cyclic voltammetry, and (c) Demodulation and reconstruction of cyclic voltammogram.

3. Results and discussion

3.1. Expression of yeast biobricks

Yeast display has advantages of high surface expression and eukaryotic protein processing mechanisms (Rosano and Ceccarelli, 2014) compared to traditional bacterial platforms. Likewise, yeast display offers advantages in the cost of reagent production as well as improved assay stability and shelf life of lyophilized cells (Gray et al., 2012). "Dual–affinity biobricks" were engineered by cloning the full length HCV core gene spanning 572 bp from HCV genotype 1 into the pYD and pCTCON2 vectors (Boder and Wittrup, 1997) with gold binding peptide repeats (6–9 ×), to yield the HCV core and GBP fusion protein linked by glycine-serine repeats to Aga1–2 and the yeast surface (Fig. 3).

These constructs create a cell-based reagent capable of concomitant surface immobilization and antibody capture. We engineered pYD6, pYD8, and pCTCON2 vectors to compare *C*- and *N*-terminal Aga-2 linkage and the effect of order (Core/GBP vs. GBP/Core) of motif expression. Gal-raffinose induction showed greater than 80% surface expression for pCTCON2 while lower and variable expression was observed for pYD6 and pYD8. Fig. 3b shows the expression efficiency of the two vector systems as measured by flow cytometry, where the control corresponds to yeast cells without the HCV core/GBP gene inserted in the transformed vector. Immuno-precipitation and fluorescent imaging of pCTCON2 yeast confirmed high surface expression and avid binding of core directed antibodies to the yeast biobrick surface (Fig. 4).

3.2. Immuno-fluorescent and electrochemical assays

Standard optical calibration assays were performed to assess the limit of detection (LOD), dynamic range (DR) and dissociation constant (K_d), of surface displayed chimera to monoclonal anti-HCV core antibodies (Fig. 5a). A LOD of 12.3 pM, DR of 30 pM–3 nM and K_d of 277 ± 37 pM were observed in optimized optical experiments. Subsequently, cyclic voltammetry was employed with yeast functionalized gold SPEs for electrochemical testing. Preliminary assays in this format provided consistent, but elevated binding parameters with a 2 nM LOD, 4–250 nM DR, and 49.94 ± 6.69 nM K_d (Fig. 4b). Individual voltammograms are shown in the Supplemental (S1). The observed differences in assay parameters between the immuno-fluorescent and electrochemical assay are attributed to signal leakage from the electrode surface, which is unmeasured in the electrochemical method but captured in bulk optical measurements. This phenomenon, attributed to the distance between the yeast surface and the sensing electrode, may be addressed by creating yeast surface monolayers or secreting protein only biobricks, methods that will be the subject of upcoming reports. The specificity of HCV core to selectively capture anti-HCV core IgG was measured for several off-target antibodies and found to have signal comparable to that when no anti-HCV core antibody is present (Supplementary S2).

3.3. Smartphone-based potentiostat

In order to demonstrate the POC utility of the electrochemical assay, a smartphone-based potentiostat was developed that can be controlled by a mobile app and interfaces with yeast biobrick functionalized SPEs for portable and accurate electrochemical measurements (Sun et al., 2014, 2016). The potentiostat interfaces with the phone through the audio jack making it universally compatible with any smartphone, regardless of make or model – unlike devices that use proprietary ports such as Lightening or USB that are only found on a subset of smartphones. This also obviates the need for replacing or recharging an external battery since the phone can provide the power. Most importantly, the audio port enables the device to take advantage of the many capabilities of the smartphone, including processing power, battery, network connectivity, and easy-to-develop software applications. This also avoids adding redundant components that are already available on the phone allowing it to be more portable and cost-effective as compared to stand-alone variants (Cruz et al., 2014; Ionescu et al., 2010; Laksanasopin et al., 2015; Lillehoj et al., 2013; Nemiroski et al., 2014; Rowe et al., 2011; Wang et al., 2015; Zhang et al., 2016).

The main challenge in using the headphone jack is that the audio channels are AC coupled meaning that no DC signal or power can be directly transmitted between the phone and the potentiostat. Hence, in order to power to the device, a sinusoidal AC signal with a frequency in the audio band (20 Hz–20 kHz) is sent through the left channel to be harvested by the device. For bidirectional digital communication, RS-232 is used with a baud rate of 2.4 kHz, which is within the audio bandwidth, allowing these packets of data to pass through the AC coupling and be decoded without additional conditioning or processing. Since CV measurements result in slow varying waveforms close to DC, the output of the potentiostat cannot be directly passed to the phone either. One solution would be to digitize this signal and send it digitally. However, this requires adding an analog to digital converter (ADC) to the device, which would increase the power consumption and cost. Instead, we push this burden back onto the phone with its far superior ADC and processing power by modulating the signal using a VCO. The analog signal from the potentiostat is translated into a frequency modulated signal within the audio band allowing it to be sent directly to the phone to be

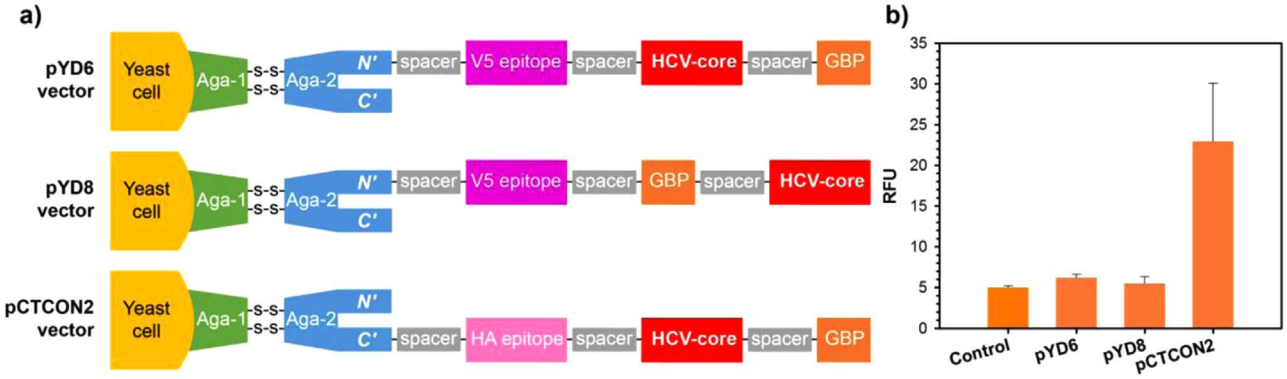

Fig. 3. Selection of expression vector for yeast cells to display HCV core protein on its surface: (a) Position of HCV core protein and gold binding peptide in the Aga1-Aga2 display system using in the pYD6, pYD8, and pCTCON2 vector systems. (b) Comparison of vector efficiency to display HCV core protein on yeast cell's surface, assayed with mouse anti-HCV core antibody.

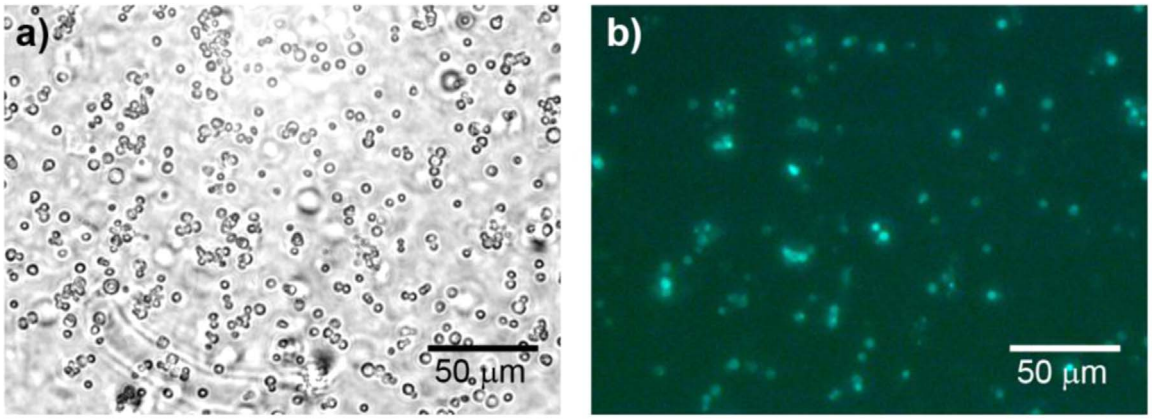

Fig. 4. Validation of HCV-core expression by immuno-fluorescent assay: (a) Bright field microscopic image of yeast cell expressing HCV core protein, (b) Fluorescent image of yeast cells expressing HCV core protein detected by HCV core directed antibody (mouse anti-HCV core and Alexa Fluor 488-anti-mouse).

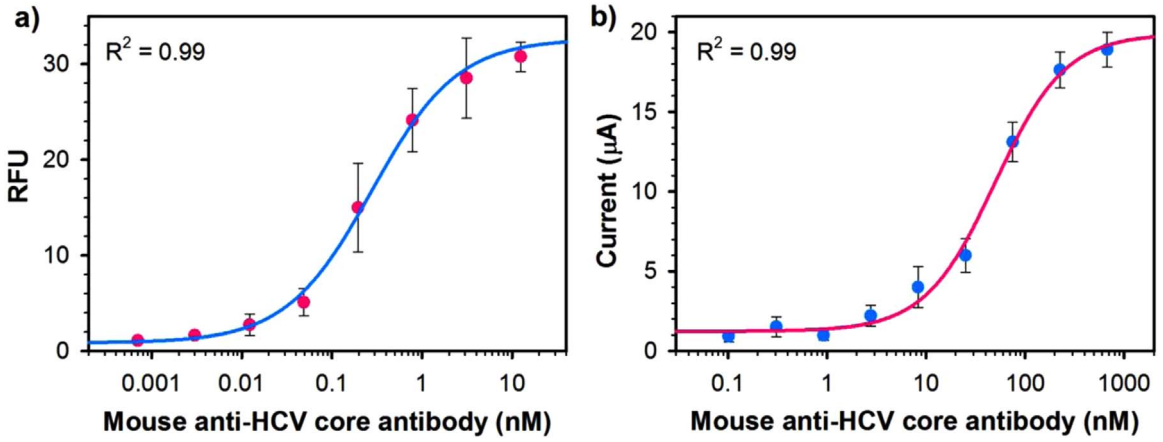

Fig. 5. Detection of mouse monoclonal anti-HCV core antibody: (a) immuno-fluorescent assay and (b) electrochemical assay with CHI electrochemical workstation. The mean and standard deviation of all concentrations were from triplicates and fitted with 4 – parameter logistic regression.

processed. This device with the power harvesting network and communication schemes can measure bidirectional currents as low as 300 pA, consumes a peak power of 6.9 mW during measurements, which is within the power budget set by the typical output of mobile devices, and harvests power with up to 79% efficiency.

The functionality of the smartphone-based potentiostat was verified by electrochemical measurement of pAP concentration, formed as a result of enzymatic conversion by ALP present in the SPE immobilized immune complex, with parallel comparison to a CHI reference platform (Fig. 6) (Sun et al., 2014). Fig. 6a shows voltammograms of the same electrodes measured consecutively by the CHI and smartphone-based potentiostat. Although the voltage scanning windows are slightly different, both data sets cover the range required to detect pAP concentration, +100 mV to +200 mV with respect to reference electrode (highlighted in gray). Shortening this range minimizes the runtime of the CV scan allowing the smartphone-based potentiostat to conserve power

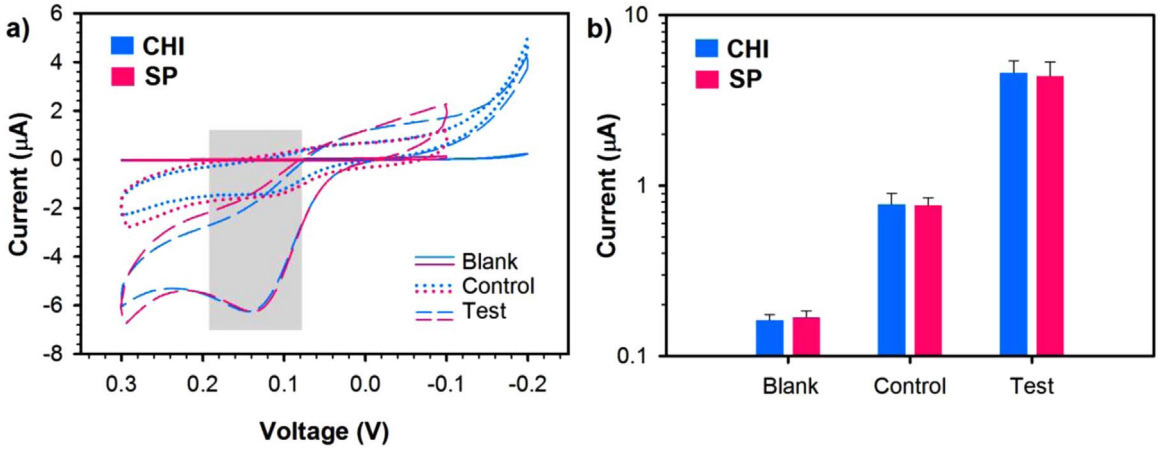

Fig. 6. Performance of smartphone-based potentiostat (SP): (a) Cyclic voltammograms and (b) Extracted peak current of CHI and SP for Blank (substrate (pAPP) on a 2% BSA blocked SPE), Control (0 nM anti-HCV antibody) and Test (100 nM anti-HCV antibody). All measurements taken in triplicate and error bars represent ± 1 standard deviation.

and reduces the measurement time. The tests labelled "Blank" represent the absolute background noise, in which only electrochemically inactive substrate (pAPP) was added to SPEs blocked only with BSA and measured by cyclic voltammetry. In both the positive (100 nM anti-HCV antibody) and control experiments, the SPEs contained all the assay components with the exception that no anti-HCV core antibody was added to the control SPEs. Direct comparison of CHI and smartphone-based potentiostat based on Bland-Altman plot (not shown) revealed 95% limits of agreement between the two instruments of +0.24 μA and −0.39 μA and an average difference of 0.074 μA. As these differences are smaller than the current signals at the LOD for the electrochemical assay (< 1 μA) as well as insignificant when compared to the peak currents of the higher concentrations (> 10 μA), these data demonstrate equivalence of both the smartphone-based potentiostat (SP) and the laboratory grade instrument (CHI) when used with biobrick-based electrochemical assays.

4. Conclusion

Here we demonstrated an integrated diagnostic approach that innovates and evolves two key areas of biomedical sensing, reagent production/preparation and connected signal acquisition/processing. We have applied this approach to the detection of HCV core-directed antibodies using dual-affinity yeast biobricks and shown these are compatible with immuno-precipitation and standard fluorescent and electrochemical assay formats. We have also demonstrated that one-step purification, enrichment, and surface immobilization can be carried out via gold monolayers on glass or screen printed surfaces and these perform as well or better than standard antibody immobilization techniques since the spherical symmetry of the system ensures a large surface area and correct orientation of antigen with respect to dissolved antibody. Moreover, the technique can be rapidly expanded to other antigens (or antibodies can be displayed or selected using yeast libraries) and large amounts of stable reagent can be produced with only minimal laboratory requirements.

In previous work we demonstrated the ability of surface expressed single chain antibodies to detect circulating antigen, whereas in this work we explored the use of antigen based antibody capture methods needed for immuno-screening. While optical experiments showed excellent sensitivity for HCV directed antibodies, electrochemical methods had elevated detection limits and would require refinement for physiologic testing. Likewise, non-specific (yeast directed) antibody binding might be expected *in vivo* and methods to increase specificity such as serum pretreatment (adsorption of non-specific antibodies with antigen-free yeast) or cell-free systems using secreted biobricks will be explored in future works.

Overall we propose that blending the renewable nature of biobricks and the scalability of electrochemical and optical sensing will promote more affordable approaches for point of care diagnostics.

Acknowledgements

This research was funded in part by the Institute for Public Health (IPH), UCSD Clinical and Translational Research Institute (UL1TR001442), Calit2 Strategic Research Opportunities (CSRO), and the UCSD Center for AIDS Research (CFAR). CFAR is an NIH-funded program (P30 AI036214), which is supported by the following NIH Institutes and centers: NIAID, NCI, NIMH, NIDA, NICHD, NHLBI, NIA, NIGMS, and NIDDK (P30 Umbrella grant). Special thanks to Dr. Chip Schooley for ongoing laboratory support.

Appendix A. Supporting information

Supplementary data associated with this article can be found in the online version at doi:10.1016/j.bios.2016.07.023.

References

Acosta-Rivero, N., Musacchio, A., Lorenzo, L., Alvarez, C., Morales, J., 2002. Processing of the Hepatitis C virus precursor protein expressed in the methylotrophic yeast Pichia pastoris. Biochem. Biophys. Res. Commun. 295, 81–84. http://dx.doi.org/10.1016/S0006-291X(02)00635-6.

Barrera, J.M., Francis, B., Ercilla, G., Nelles, M., Achord, D., Darner, J., Lee, S.R., 1995. Improved detection of anti-HCV in post-transfusion hepatitis by a third-generation ELISA. Vox Sang. 68, 15–18.

Baumert, T.F., Ito, S., Wong, D.T., Liang, T.J., 1998. Hepatitis C virus structural proteins assemble into viruslike particles in insect cells. J. Virol. 72, 3827–3836.

Boder, E.T., Wittrup, K.D., 1997. Yeast surface display for screening combinatorial polypeptide libraries. Nat. Biotechnol. 15, 553–557. http://dx.doi.org/10.1038/nbt0697-553.

Bouvier-Alias, M., Patel, K., Dahari, H., Beaucourt, S., Larderie, P., Blatt, L., Hezode, C., Picchio, G., Dhumeaux, D., Neumann, A.U., McHutchison, J.G., Pawlotsky, J.-M., 2002. Clinical utility of total HCV core antigen quantification: a new indirect marker of HCV replication. Hepatology 36, 211–218. http://dx.doi.org/10.1053/jhep.2002.34130.

Chen, S.L., Morgan, T.R., 2006. The natural history of Hepatitis C Virus (HCV) infection. Int. J. Med. Sci. 3, 47–52. http://dx.doi.org/10.7150/ijms.3.47.

Cherf, G.M., Cochran, J.R., 2015. Applications of yeast surface display for protein engineering. Methods Mol. Biol. 1319, 155–175. http://dx.doi.org/10.1007/978-1-4939–2748-7_8.

Cruz, A.F.D., Norena, N., Kaushik, A., Bhansali, S., 2014. A low-cost miniaturized potentiostat for point-of-care diagnosis. Biosens. Bioelectron. 62, 249–254. http://dx.doi.org/10.1016/j.bios.2014.06.053.

Du, C., Chan, W.C., McKeithan, T.W., Nickerson, K.W., 2005. Surface display of recombinant proteins on *Bacillus thuringiensis* spores. Appl. Environ. Microbiol. 71, 3337–3341. http://dx.doi.org/10.1128/AEM.71.6.3337–3341.2005.

Edlin, B.R., Winkelstein, E.R., 2014. Can hepatitis C be eradicated in the United States? Antivir. Res. 110, 79–93. http://dx.doi.org/10.1016/j.antiviral.2014.07.015.

Gaudy, C., Thevenas, C., Tichet, J., Mariotte, N., Goudeau, A., Dubois, F., 2005. Usefulness of the hepatitis C virus core antigen assay for screening of a population undergoing routine medical checkup. J. Clin. Microbiol. 43, 1722–1726. http://dx.doi.org/10.1128/JCM.43.4.1722–1726.2005.

Graham, C.S., Swan, T., 2015. A path to eradication of hepatitis C in low- and middle-income countries. Antivir. Res. 119, 89–96. http://dx.doi.org/10.1016/j.antiviral.2015.01.004.

Gray, S.A., Weigel, K.M., Ali, I.K.M., Lakey, A.A., Capalungan, J., Domingo, G.J., Cangelosi, G.A., 2012. Toward low-cost affinity reagents: lyophilized yeast-scfv probes specific for pathogen antigens. PLoS One 7, e32042. http://dx.doi.org/10.1371/journal.pone.0032042.

Gretch, D.R., 1997. Diagnostic tests for hepatitis C. Hepatology 26, 43S–47S. http://dx.doi.org/10.1002/hep.510260708.

Hagan, L.M., Schinazi, R.F., 2013. Best strategies for global HCV eradication. Liver Int. 33, 68–79. http://dx.doi.org/10.1111/liv.12063.

Harada, S., Watanabe, Y., Takeuchi, K., Suzuki, T., Katayama, T., Takebe, Y., Saito, I., Miyamura, T., 1991. Expression of processed core protein of hepatitis C virus in mammalian cells. J. Virol. 65, 3015–3021.

Ionescu, C., Svasta, P., Tamas, C., Bala, C., Rotariu, L., 2010. Portable measuring and display unit for electrochemical sensors, in: Proceedings of the 16th International Symposium IEEE for Design and Technology in Electronic Packaging (SIITME), 2010. Presented at the Design and Technology in Electronic Packaging (SIITME). 20, pp. 215–218. http://dx.doi.org/10.1109/SIITME.2010.5653021.

Iwanicki, A., Piątek, I., StasiłojĆ, M., Grela, A., Łęga, T., Obuchowski, M., Hinc, K., 2014. A system of vectors for *Bacillus subtilis* spore surface display. Microb. Cell Factor. 13, 30. http://dx.doi.org/10.1186/1475–2859-13-30.

Juan-Franco, E., de, Caruz, A., Pedrajas, J.R., Lechuga, L.M., 2013. Site-directed antibody immobilization using a protein A–gold binding domain fusion protein for enhanced SPR immunosensing. Analyst 138, 2023–2031. http://dx.doi.org/10.1039/C3AN36498D.

Kao, J.H., Lai, M.Y., Hwang, Y.T., Yang, P.M., Chen, P.J., Sheu, J.C., Wang, T.H., Hsu, H.C., Chen, D.S., 1996. Chronic hepatitis C without anti-hepatitis C antibodies by second-generation assay. A clinicopathologic study and demonstration of the usefulness of a third-generation assay. Dig. Dis. Sci. 41, 161–165.

Kuo, G., Choo, Q.L., Alter, H.J., Gitnick, G.L., Redeker, A.G., Purcell, R.H., Miyamura, T., Dienstag, J.L., Alter, M.J., Stevens, C.E., 1989. An assay for circulating antibodies to a major etiologic virus of human non-A, non-B hepatitis. Science 244, 362–364.

Laksanasopin, T., Guo, T.W., Nayak, S., Sridhara, A.A., Xie, S., Olowookere, O.O., Cadinu, P., Meng, F., Chee, N.H., Kim, J., Chin, C.D., Munyazesa, E., Mugwaneza, P., Rai, A.J., Mugisha, V., Castro, A.R., Steinmiller, D., Linder, V., Justman, J.E.,

Nsanzimana, Q., Sia, S.K., 2015. A smartphone dongle for diagnosis of infectious diseases at the point of care. Sci. Transl. Med. 7. http://dx.doi.org/10.1126/scitranslmed.aaa0056, 273re1–273re1.

Lillehoj, P.B., Huang, M.-C., Truong, N., Ho, C.-M., 2013. Rapid electrochemical detection on a mobile phone. Lab Chip 13, 2950–2955. http://dx.doi.org/10.1039/C3LC50306B.

Madesis, P., Osathanunkul, M., Georgopoulou, U., Gisby, M.F., Mudd, E.A., Nianiou, I., Tsitoura, P., Mavromara, P., Tsaftaris, A., Day, A., 2010. A hepatitis C virus core polypeptide expressed in chloroplasts detects anti-core antibodies in infected human sera. J. Biotechnol. 145, 377–386. http://dx.doi.org/10.1016/j.jbiotec.2009.12.001.

Majeau, N., Gagné, V., Boivin, A., Bolduc, M., Majeau, J.-A., Ouellet, D., Leclerc, D., 2004. The N-terminal half of the core protein of hepatitis C virus is sufficient for nucleocapsid formation. J. Gen. Virol. 85, 971–981. http://dx.doi.org/10.1099/vir.0.79775-0.

Nemiroski, A., Christodouleas, D.C., Hennek, J.W., Kumar, A.A., Maxwell, E.J., Fernández-Abedul, M.T., Whitesides, G.M., 2014. Universal mobile electrochemical detector designed for use in resource-limited applications. Proc. Natl. Acad. Sci. 111, 11984–11989. http://dx.doi.org/10.1073/pnas.1405679111.

Park, Y., Lee, J.-H., Kim, B.S., Kim, D.Y., Han, K.-H., Kim, H.-S., 2010. New automated hepatitis C virus (HCV) core antigen assay as an alternative to real-time PCR for HCV RNA quantification. J. Clin. Microbiol. 48, 2253–2256. http://dx.doi.org/10.1128/JCM.01856-09.

Qin, J., Wang, X., Kong, J., Ma, C., Xu, P., 2014. Construction of a food-grade cell surface display system for *Lactobacillus casei*. Microbiol. Res. 169, 733–740. http://dx.doi.org/10.1016/j.micres.2014.02.001.

Ribeiro, R.M., Li, H., Wang, S., Stoddard, M.B., Learn, G.H., Korber, B.T., Bhattacharya, T., Guedj, J., Parrish, E.H., Hahn, B.H., Shaw, G.M., Perelson, A.S., 2012. Quantifying the diversification of Hepatitis C Virus (HCV) during primary infection: estimates of the in vivo mutation rate. Plos Pathog. 8, e1002881. http://dx.doi.org/10.1371/journal.ppat.1002881.

Rosano, G.L., Ceccarelli, E.A., 2014. Recombinant protein expression in *Escherichia coli*: advances and challenges. Front. Microbiol., 5. http://dx.doi.org/10.3389/fmicb.2014.00172.

Rouet, F., Deleplancque, L., Mboumba, B.B., Sica, J., Mouinga-Ondémé, A., Liégeois, F., Goudeau, A., Dubois, F., Gaudy-Graffin, C., 2015. Usefulness of a fourth generation ELISA assay for the reliable identification of HCV infection in HIV-positive adults from gabon (Central Africa). PLoS ONE, 10. http://dx.doi.org/10.1371/journal.pone.0116975.

Rowe, A.A., Bonham, A.J., White, R.J., Zimmer, M.P., Yadgar, R.J., Hobza, T.M., Honea, J.W., Ben-Yaacov, I., Plaxco, K.W., 2011. CheapStat: an open-source, "Do-It-Yourself" potentiostat for analytical and educational applications. PLoS One 6, e23783. http://dx.doi.org/10.1371/journal.pone.0023783.

Saito, I., Miyamura, T., Ohbayashi, A., Harada, H., Katayama, T., Kikuchi, S., Watanabe, Y., Koi, S., Onji, M., Ohta, Y., 1990. Hepatitis C Virus infection is associated with the development of hepatocellular carcinoma. Proc. Natl. Acad. Sci. USA 87, 6547–6549.

Sehr, P., Müller, M., Höpfl, R., Widschwendter, A., Pawlita, M., 2002. HPV antibody detection by ELISA with capsid protein L1 fused to glutathione S-transferase. J. Virol. Methods 106, 61–70. http://dx.doi.org/10.1016/S0166-0934(02)00134-9.

Stanley, B., 1997. Metal-recognition by repeating polypeptides. Nat. Biotechnol. 15, 269–272. http://dx.doi.org/10.1038/nbt0397-269.

Stoll-Keller, F., Barth, H., Fafi-Kremer, S., Zeisel, M.B., Baumert, T.F., 2009. Development of hepatitis C virus vaccines: challenges and progress. Expert Rev. Vaccin. 8, 333–345. http://dx.doi.org/10.1586/14760584.8.3.333.

Sun, A., Wambach, T., Venkatesh, A.G., Hall, D.A., 2014. A Low-Cost Smartphone-based Electrochemical Biosensor for Point-of-Care Diagnostics, in: Proceedings of the IEEE Biomedical Circuits and Systems Conference (BioCAS) 2014. Presented at the 2014 IEEE Biomedical Circuits and Systems Conference (BioCAS), pp. 312–315. http://dx.doi.org/10.1109/BioCAS.2014.6981725.

Sun, A.C., Yao, C., Venkatesh, A.G., Hall, D.A., 2016. An efficient power harvesting mobile phone-based electrochemical biosensor for point-of-care health monitoring. Sens. Actuators B: Chem. 235, 126–135.

Suthar, A.B., Harries, A.D., 2015. A public health approach to hepatitis C control in low- and middle-income countries. PLoS Med. 12, e1001795. http://dx.doi.org/10.1371/journal.pmed.1001795.

Uliana, C.V., Riccardi, C.S., Yamanaka, H., 2014. Diagnostic tests for hepatitis C: recent trends in electrochemical immunosensor and genosensor analysis. World J. Gastroenterol. 20, 15476–15491. http://dx.doi.org/10.3748/wjg.v20.i42.15476.

Uyttendaele, S., Claeys, H., Mertens, W., Verhaert, H., Vermylen, C., 1994. Evaluation of third-generation screening and confirmatory assays for HCV antibodies. Vox Sang. 66, 122–129. http://dx.doi.org/10.1111/j.1423–0410.1994.tb00293.x.

van Bloois, E., Winter, R.T., Kolmar, H., Fraaije, M.W., 2011. Decorating microbes: surface display of proteins on *Escherichia coli*. Trends Biotechnol. 29, 79–86. http://dx.doi.org/10.1016/j.tibtech.2010.11.003.

Venkatesh, A.G., Sun, A., Brickner, H., Looney, D., Hall, D.A., Aronoff-Spencer, E., 2015. Yeast dual-affinity biobricks: progress towards renewable whole-cell biosensors. Biosens. Bioelectron. 70, 462–468. http://dx.doi.org/10.1016/j.bios.2015.03.044.

Wang, X., Gartia, M.R., Jiang, J., Chang, T.-W., Qian, J., Liu, Y., Liu, X., Liu, G.L., 2015. Audio jack based miniaturized mobile phone electrochemical sensing platform. Sens. Actuators B Chem. 209, 677–685. http://dx.doi.org/10.1016/j.snb.2014.12.017.

Wang, Z., Mathias, A., Stavrou, S., Neville, D.M., 2005. A new yeast display vector permitting free scFv amino termini can augment ligand binding affinities. Protein Eng. Des. Sel. 18, 337–343. http://dx.doi.org/10.1093/protein/gzi036.

Yao, C., Sun, A., Hall, D.A., 2015. Efficient power harvesting from the mobile phone audio jack for mHealth peripherals, in: Proceedings of the 2015 IEEE Global Humanitarian Technology Conference (GHTC). Presented at the 2015 IEEE Global Humanitarian Technology Conference (GHTC), pp. 219–225. doi:10.1109/GHTC.2015.7343976.

Zanetti, A.R., Romanò, L., Brunetto, M., Colombo, M., Bellati, G., Tackney, C., 2003. Total HCV core antigen assay: a new marker of hepatitis C viremia for monitoring the progress of therapy. J. Med. Virol. 70, 27–30. http://dx.doi.org/10.1002/jmv.10355.

Zhang, D., Lu, Y., Zhang, Q., Liu, L., Li, S., Yao, Y., Jiang, J., Liu, G.L., Liu, Q., 2016. Protein detecting with smartphone-controlled electrochemical impedance spectroscopy for point-of-care applications. Sens. Actuators B Chem. 222, 994–1002. http://dx.doi.org/10.1016/j.snb.2015.09.041.